Temperature dependence of the interlayer magnetoresistance of quasi-one-dimensional Fermi liquids at the magic angles

2000 J. Phys.: Condens. Matter 12 7945

(http://iopscience.iop.org/0953-8984/12/36/309)

J. Phys.: Condens. Matter **12** (2000) 7945–7956. Printed in the UK PII: S0953-8984(00)14800-3

Temperature dependence of the interlayer magnetoresistance of quasi-one-dimensional Fermi liquids at the magic angles

Ross H McKenzie† and Perez Moses

School of Physics, University of New South Wales, Sydney 2052, Australia

E-mail: mckenzie@physics.uq.edu.au

Received 19 June 2000

Abstract. The interlayer magnetoresistance of a quasi-one-dimensional Fermi liquid is considered for the case of a magnetic field that is rotated within the plane perpendicular to the most-conducting direction. Within semi-classical transport theory, dips in the magnetoresistance occur at integer 'magic angles' only when the electronic dispersion parallel to chains is non-linear. If the field direction is fixed at one of the magic angles and the temperature is varied, then the resulting variation of the scattering rate can lead to a non-monotonic variation of the interlayer magnetoresistance with temperature. Although the model considered here gives a good description of some of the properties of the Bechgaard salts, $(TMTSF)_2PF_6$ for pressures less than 8 kbar and $(TMTSF)_2ClO_4$, it gives a poor description of their properties when the field is parallel to the layers and of the intralayer transport.

1. Introduction

In spite of intensive research over the past decade, the nature of the metallic state in low-dimensional strongly correlated materials is still poorly understood. Widely studied materials include cuprate and organic superconductors [1, 2]. Many of the properties of the cuprates cannot be understood within the Fermi-liquid picture that has so successfully described conventional metals [3]. Although some properties of the quasi-two-dimensional molecular crystals κ-(BEDT-TTF)$_2$X [4] and the quasi-one-dimensional Bechgaard salts [5] (TMTSF)$_2$X can be explained within a Fermi-liquid framework, others cannot. A particular challenge is understanding the dependence of the magnetoresistance of the Bechgaard salts on the direction of the magnetic field, especially $(TMTSF)_2PF_6$ under pressures of about 10 kbar [6,7]. The different angle-dependent magnetoresistance effects in quasi-one-dimensional metals are known as the Danner [8], magic angle (or Lebed) [9–14], and third-angular effects [15], depending on whether the magnetic field is rotated in the $\boldsymbol{a}$–$\boldsymbol{c}$, $\boldsymbol{b}$–$\boldsymbol{c}$, or $\boldsymbol{a}$–$\boldsymbol{b}$ plane, respectively. (The most- and least-conducting directions are those of the $\boldsymbol{a}$- and $\boldsymbol{c}$-axes, respectively.) The magic angle effect is the most poorly understood of these effects and is the focus of this paper. If θ is the angle between the magnetic field and the $\boldsymbol{c}$-axis, then at the 'magic angles' given by

$$\tan\theta = \frac{b}{c}\frac{p}{q} \qquad \pm p, q = 1, 2, 3, \ldots \tag{1}$$

where b and c are the lattice constants in the $\boldsymbol{b}$- and $\boldsymbol{c}$-directions, Lebed predicted dips in the threshold field for formation of a field-induced spin-density wave [9]. Although these dips

† New address: Department of Physics, University of Queensland, St Lucia, 4072, Australia.

0953-8984/00/367945+12$30.00

are not observed [10], features are seen, mostly at $p/q = 1, 2$ in the torque [12] and in all components of the resistance [7, 12–14, 16–18].

A wide range of physical mechanisms have been proposed to explain these effects including commensurability effects changing the electron–electron scattering rate [11], semi-classical transport [19], complicated band structures [20, 21], hot spots on the Fermi surface [22], cold spots on the Fermi surface [23], electron–electron interactions [24], non-Fermi-liquid effects [25], and changes in effective dimensionality induced by magnetic fields [26].

The properties of $(TMTSF)_2PF_6$ at 10 kbar are particularly difficult to understand. For example, when the magnetic field is perpendicular to the current direction, the magnetoresistance is smaller than when it is parallel, the opposite of what one observes for $(TMTSF)_2ClO_4$ and for conventional metals. Recently, the temperature dependence of the magnetoresistance when the field direction was fixed at the first magic angle was measured [7]. It was found to be non-monotonic: as the temperature decreased down to T_{min}, the magnetoresistance decreased; it increased until T_{max} was reached, and then decreased. It has recently been proposed that these two temperatures actually represent phase transitions between metallic and insulating phases [26]. The magnetoresistance of the quasi-two-dimensional metal α-$(BEDT\text{-}TTF)_2MHg(SCN)_4$ (M = K, Rb, Tl) also exhibits unusual temperature and angular dependence [27, 28].

The purpose of this paper is to clarify what properties of the magic angle effects can only be explained within a non-Fermi-liquid framework by seeing what effects can be explained within Fermi-liquid theory. The interlayer magnetoresistance is calculated within the framework of semi-classical transport theory. It is found that if one takes into account the finite bandwidth along the most-conducting direction, then dips in the magnetoresistance are observed for $p/q = 1, 2, 3, \ldots$ [19]. Furthermore, if one assumes a simple Fermi-liquid form for the temperature dependence of the scattering rate, then at the magic angles the interlayer magnetoresistance does have a non-monotonic temperature dependence. Hence, one should be cautious about associating maxima and minima in the temperature dependence with metal–insulator transitions. However, the results obtained give a poor description of the observed properties when the field is close to the ***b***-axis and of the resistivity within the layers.

2. Calculation of the interlayer conductivity

2.1. Semi-classical transport theory

If the electronic dispersion relation is $\epsilon(\vec{k})$ then the electronic group velocity perpendicular to the layers is $v_z = (1/\hbar)\,\partial\epsilon(\vec{k})/\partial k_z$. The interlayer conductivity can be calculated by solving the Boltzmann equation in the relaxation time approximation leading to Chambers' formula [29]

$$\sigma_{zz} = \frac{e^2\tau}{4\pi^3}\int v_z(\vec{k})\bar{v}_z(\vec{k})\left(-\frac{\partial f(\epsilon)}{\partial\epsilon}\right)\mathrm{d}^3\vec{k} \tag{2}$$

where $f(\epsilon)$ is the Fermi function and τ is the scattering time which is assumed to be the same at all points on the Fermi surface. $\bar{v}_z(\vec{k})$ is the electron velocity averaged over its trajectories on the Fermi surface:

$$\bar{v}_z(\vec{k}) = \frac{1}{\tau}\int_{-\infty}^{0}\exp\left(\frac{t}{\tau}\right)v_z(\vec{k}(t))\,\mathrm{d}t \tag{3}$$

where $\vec{k}(0) = \vec{k}$. The time dependence of the wave vector $\vec{k}(t)$ is found by integrating the semi-classical equation of motion

$$\frac{\mathrm{d}\vec{k}}{\mathrm{d}t} = -\frac{e}{\hbar^2}\,\vec{\nabla}_k\epsilon \times \vec{B}. \tag{4}$$

If the temperature is sufficiently low that $T \ll E_F$, then $\partial f/\partial\epsilon$ in equation (2) can be replaced by a delta function at the Fermi energy and equation (2) becomes

$$\sigma_{zz} = \frac{e^2\tau}{4\pi^3}\int v_z(\vec{k})\bar{v}_z(\vec{k})\delta(E_F - \epsilon(\vec{k}))\,\mathrm{d}^3\vec{k}. \tag{5}$$

2.2. Dispersion relation along the chains

In the tight-binding approximation the dispersion relation for an orthorhombic crystal can be written as

$$\epsilon(\vec{k}) = -2t_a\cos(k_x a) - 2t_b\cos(k_y b) - 2t_c\cos(k_z c) \tag{6}$$

where t_a, t_b, and t_a are the intersite hopping integrals along the different crystal axes. For the Bechgaard salts, $t_a \gg t_b, t_c$, the dispersion along the chains can be linearized giving

$$\epsilon(\vec{k}) = \hbar v_F(|k_x| - k_F) - 2t_b\cos(bk_y) - 2t_c\cos(bk_z)$$

where $v_F = 2t_a a\sin(ak_F)/\hbar$ is the Fermi velocity and k_F is the Fermi wave vector. This linear dispersion has been used in a number of papers on the magic angle effect [20–22, 24]. If one solves for the interlayer conductivity within semi-classical transport theory, one obtains

$$\frac{\sigma_{zz}(\theta)}{\sigma^0_{zz}} = \frac{1}{1 + (\omega_{c0}\tau\sin\theta)^2} \tag{7}$$

where $\omega_{c0} = ev_F cB/\hbar$ is the frequency at which an electron traverses the Brillouin zone in the $\boldsymbol{c}$-direction when the field is parallel to the $\boldsymbol{b}$-axis. Clearly this is a smoothly varying function of θ and does not exhibit any magic angle effects.

We now show that if the full non-linear dispersion (6) is used, then one does obtain magic angle effects. We will re-derive a result obtained earlier by Maki [19] with a view to elucidating the physics in the process.

2.3. Solution of the semi-classical equations of motion

The group velocity for the dispersion relation (6) is

$$\vec{v}(\vec{k}) = \frac{1}{\hbar}\vec{\nabla}_k\epsilon = \frac{1}{\hbar}\begin{pmatrix} 2at_a\sin(ak_x) \\ 2bt_b\sin(bk_y) \\ 2ct_c\sin(ck_z)\end{pmatrix}. \tag{8}$$

The rate of change of the wave vector $\vec{k}(t)$, in a magnetic field in the $\boldsymbol{b}$–$\boldsymbol{c}$ plane, $\vec{B} = (0, B\sin\theta, B\cos\theta)$, is given by (4)

$$\frac{\mathrm{d}\vec{k}}{\mathrm{d}t} = \frac{1}{\hbar^2}\begin{pmatrix} -2beBt_b\cos\theta\sin(bk_y) \\ 2aeBt_a\cos\theta\sin(ak_x) \\ -2aeBt_a\sin\theta\sin(ak_x)\end{pmatrix} \tag{9}$$

where terms involving t_c have been neglected. This is valid provided that $t_c\sin\theta \ll t_b\cos\theta$. Hence, the results below will not be valid as $\theta \to 90^\circ$.

In order to calculate the z-component of the velocity, one needs to obtain $\vec{k}_z(t)$, which the bottom line of equation (9) shows is determined by $k_x(t)$. To zeroth order in t_b, $k_x(t) = k_F$. Integrating the middle line of equation (9) then gives

$$k_y(t) = k_y(0) + \frac{\omega_b}{b}t \tag{10}$$

where

$$\omega_b = v_F eBb\cos\theta/\hbar \equiv \omega_{b0}\cos\theta \tag{11}$$

is the frequency at which an the electron traverses the Brillouin zone in the direction of the $\boldsymbol{b}$-axis.

Substituting this into the top line of equation (9) and integrating gives, to first order in t_b/t_a,

$$k_x(t) = k_F + \frac{2t_b}{\hbar v_F}\cos(bk_y(0) + \omega_b t). \tag{12}$$

We obtain $k_z(t)$ by using the bottom line of equation (9) and substituting in (12), giving

$$\frac{\mathrm{d}k_z}{\mathrm{d}t} = \frac{-2aeBt_a\sin\theta}{\hbar^2}\left[\sin(k_F)\cos\left(\frac{2at_b}{\hbar v_F}\cos(bk_y(0)+\omega_b t)\right)\right.$$
$$\left. + \cos(ak_F)\sin\left(\frac{2at_b}{\hbar v_F}\cos(bk_y(0)+\omega_b t)\right)\right] \tag{13}$$

where we have used trigonometric identities to expand $\sin(ak_x(t))$. If we take a linear dispersion relation, the second term in (13) will equal zero and we are left with $\mathrm{d}k_z/\mathrm{d}t = -Bev_F\sin\theta/\hbar$, where we have assumed that at $t = 0$, the wave vector in the x-direction (k_x) is equal to k_F.

Now to first order in t_b/t_a,

$$\frac{\mathrm{d}k_z}{\mathrm{d}t} = \frac{-2aeBt_a\sin\theta}{\hbar^2}\left[\sin(ak_F) + \cos(ak_F)\sin\left(\frac{2at_b}{\hbar v_F}\cos(bk_y(0)+\omega_b t)\right)\right]. \tag{14}$$

Integrating this we obtain

$$k_z(t)c = k_z(0)c - \omega_c t - \gamma_0\tan\theta\sin(bk_y(0)+\omega_b t) \tag{15}$$

where

$$\omega_c = \omega_{c0}\sin\theta \tag{16}$$

and

$$\gamma_0 = \frac{2ct_b}{\hbar v_F}\frac{a}{b}\cot(ak_F). \tag{17}$$

2.4. Evaluation of the interlayer conductivity

Substitution of (15) into the z-component of the velocity gives

$$v_z(k_z(0),\phi,\phi') = \frac{2ct_c}{\hbar}\sin\left(ck_z(0) + \frac{\omega_c}{\omega_b}\phi' - \gamma_0\tan\theta\sin(\phi-\phi')\right) \tag{18}$$

where $\phi' = -\omega_b t$, $\phi = bk_y(0)$.

The interlayer conductivity given by (5) can then be written in the form

$$\sigma_{zz} = \frac{e^2}{4\pi^3 b\hbar v_F}\int_{-\pi/c}^{\pi/c}\mathrm{d}k_z(0)\int_0^{2\pi}\mathrm{d}\phi\; v_z(k_z(0),\phi)\int_0^{\infty}\frac{\mathrm{d}\phi'}{\omega_b}\exp\left(\frac{\phi'}{\tau\omega_b}\right)v_z(k_z(0),\phi,\phi'). \tag{19}$$

We now expand equation (18) using trigonometric identities and substitute the Bessel generating functions to obtain

$$v_z(k_z(0),\phi,\phi') = \frac{2ct_c}{\hbar}\left[\sin\left(ck_z(0)+\frac{\omega_c}{\omega_b}\phi'\right)\right.$$
$$\times\left[J_0(\gamma_0\tan\theta) + 2\sum_{k=1}^{\infty}J_{2k}(\gamma_0\tan\theta)\cos((2k)(\phi-\phi'))\right]$$
$$\left. + \cos\left(ck_z(0)+\frac{\omega_C}{\omega_b}\phi'\right)\left[2\sum_{k=0}^{\infty}J_{2k+1}(\gamma_0\tan\theta)\sin((2k+1)(\phi-\phi'))\right]\right] \tag{20}$$

and $v_z(k_z(0), \phi)$ is obtained by setting $\phi' = 0$. Substituting these expressions into equation (19) and performing the integrals over ϕ', ϕ, and $\mathrm{d}k_z(0)$, the final expression for the conductivity becomes

$$\sigma_{zz}(\theta) = \sigma_{zz}^0 \left[\frac{J_0(\gamma_0 \tan\theta)^2}{1 + (\omega_c \tau)^2} + \sum_{\nu=1}^{\infty} J_\nu(\gamma_0 \tan\theta)^2 \left(\frac{1}{1 + \tau^2(\omega_c - \omega_b \nu)^2} + \frac{1}{1 + \tau^2(\omega_c + \omega_b \nu)^2} \right) \right] \tag{21}$$

where

$$\sigma_{zz}^0 = \frac{2e^2 \tau c t_c^2}{\pi b \hbar^3 v_F}$$

is the interlayer conductivity in zero field. Note that for fixed ν and $z \ll 1$,

$$J_\nu(z) \approx \frac{(z/2)^\nu}{\Gamma(\nu + 1)}. \tag{22}$$

Maki [19] obtained a similar result, although he included the corrections to ω_b and ω_c to the next order in $(t_b/t_a)^2$. This raises the general question of to what order in t_b/t_a the above expression for σ_{zz} is valid. We only calculated $k_z(t)$ to first order in t_b/t_a. Strictly speaking, this means that (21) is valid to second order in t_b/t_a. However, we anticipate that a general solution for $v_z(t)$ will be of the form

$$v_z(t) \sim \sin(\omega_c t) \sum_n a_n \sin(\omega_b t)$$

where a_n is of order $(t_b/t_a)^n$. This means that the coefficients in (21) for $\nu \geqslant 2$ will change but be of the same order.

3. Magic angles

The angular dependence of the interlayer resistivity given by equation (21) is shown in figure 1 for several parameter values. Dips occur at the 'magic angles' given by $\omega_c = \nu \omega_b$ or

$$\tan\theta = \frac{b}{c}\,\nu \qquad \pm \nu = 1, 2, 3, \ldots \tag{23}$$

where b and c are lattice constants. The size of the dip at the νth magic angle, compared to the background magnetoresistance, will be of order

$$\left(\frac{\gamma_0}{2} \frac{b}{c} \nu \right)^{2\nu} \left(\frac{\omega_c \tau}{\nu!} \right)^2. \tag{24}$$

The size of the dips is determined by the parameter γ_0, defined by (17), which is determined by the geometry of the Fermi surface. Note that if $\gamma_0 \to 0$, equation (21) reduces to (7). This is because the limit $\gamma_0 \to 0$ corresponds to taking a linear dispersion relation. If $\gamma_0 \ll 1$, then the dips will decrease in magnitude rapidly with increasing ν. For example, if $\gamma_0 \sim 0.1$, then the $\nu = 1$ feature will be five orders of magnitude smaller than the $\nu = 3$ feature. Note that when ν becomes sufficiently large, this will no longer be valid, because $\gamma_0 \tan\theta \sim 1$.

We now consider what is a realistic value for γ_0 for the $(TMTSF)_2X$ materials. If we look at the form of γ_0 in equation (17), we note that the factor $2ct_b/(\hbar v_F)$ equals the parameter γ which determines the periodicity of the Danner oscillations [8, 30]. For $(TMTSF)_2ClO_4$ it was estimated to be 0.24. The lattice constants for $(TMTSF)_2PF_6$ are $a = 7.3$ Å, $b = 7.7$ Å, and $c = 13.5$ Å, while for $(TMTSF)_2ClO_4$, b is twice as large due to anion ordering [2]. The $\cot(ak_F)$ term depends on the band filling. At three-quarter filling, $k_F = 3\pi/(4a)$, and $\cot(ak_F) = 1$. This gives a value for $\gamma_0(PF_6) = 0.24$ and $\gamma_0(ClO_4) = 0.12$. Note that for

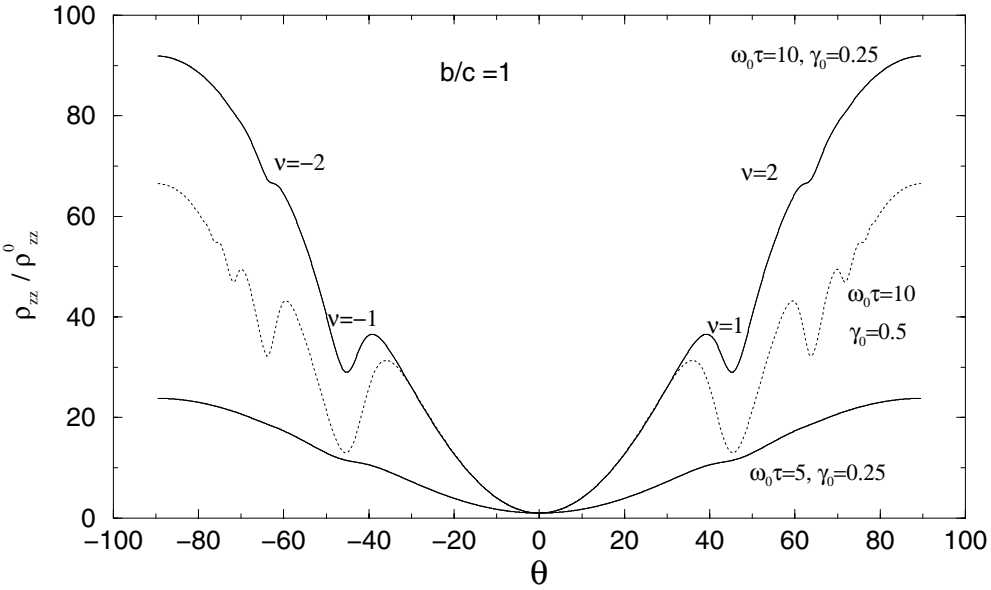

Figure 1. The angular dependence of the interlayer magnetoresistance of a quasi-one-dimensional Fermi liquid. θ is the angle between the magnetic field and the $\boldsymbol{c}$-axis and the magnetic field is rotated in the $\boldsymbol{b}$–$\boldsymbol{c}$ plane. The dips in the resistivity occur at the magic angles defined by $\tan\theta = \nu$ where $\nu = 1$ and 2 (see equation (23)). The dips only occur when one takes into account the non-linear dispersion parallel to the chains and their intensity depends on γ_0, which is determined by the geometry of the Fermi surface (equation (17)). τ is the scattering time and ω_0 is the frequency at which the electron traverses the Fermi surface when the field is perpendicular to the layers. The lattice constants b and c are set equal and so $\omega_0 = \omega_{b0} = \omega_{c0}$. The resistivity is normalized to ρ^0_{zz}, the interlayer resistivity at zero magnetic field.

half-filling, $k_F = \pi/(2a)$, and thus $\gamma_0 = 0$ and there will be no magic angle effects unless we solve the semi-classical equations to higher order in t_b.

Figure 1 is qualitatively similar to experimental results for $(TMTSF)_2ClO_4$ at ambient pressure [16] and at 6.0 kbar [17] and $(TMTSF)_2PF_6$ at 6.0 kbar (0.3 K and 4 T) [18]. A small difference is that the experimental data show a small dip near 90°, whereas the theoretical curve shows no such dip. It is quite possible that the small dips can be explained within semi-classical transport theory if one includes the effect of a finite t_c in the solution of the semi-classical transport equations. An analogous effect occurs when the field is rotated in the $\boldsymbol{a}$–$\boldsymbol{c}$ plane: for coherent interlayer transport with finite t_c, a peak in the angle-dependent magnetoresistance occurs when the field is parallel to the $\boldsymbol{a}$-axis [31].

The angular dependence of the interlayer magnetoresistance of $(TMTSF)_2PF_6$ at pressures of about 10 kbar is quite different from that shown in figure 1 At fields less than one tesla the angular dependence is similar to that given by equation (7). However, above one tesla, $\rho_{zz} \sim (B\cos\theta)^{1.3}$ and so a large dip is observed near 90°, and at 90° the in-field resistance is comparable to the zero-field resistance [7].

A number of theoretical papers [11,20–22] have predicted effects when $\tan\theta = (b/c)\,p/q$ where p/q is a fraction. In contrast, the model considered here only gives effects for $q = 1$. A review of the experimental literature shows that the only reproducible fractional features seen have been in $(TMTSF)_2ClO_4$ at $p/q = 3/2$ and $5/2$ [12]. This can be explained within the framework considered here. If $(TMTSF)_2ClO_4$ is slowly cooled, anion ordering occurs and the lattice constant in the $\boldsymbol{b}$-direction doubles, so in (23), b should be replaced by $2b$.

However, for a sample which is not completely anion ordered, it will produce features at angles corresponding to half-integers for a fully anion-ordered sample.

4. Temperature dependence of the interlayer magnetoresistance at the magic angles

Suppose that the field direction is fixed at a magic angle and the temperature (and thus the scattering time τ) is varied.

4.1. The first magic angle ($\nu = 1$)

Setting $\omega_c = \omega_b$ and using the fact that $\gamma \ll 1$ to take just the first term in the series, i.e. $\nu = 1$, the conductivity is

$$\sigma_{zz}(\theta_1) \simeq A\tau\left[\frac{1}{1+(\omega_{c0}\sin\theta_1\tau)^2} + \left(\frac{\gamma_0\tan\theta_1}{2}\right)^2\right] \tag{25}$$

where θ_1 represents the first magic angle and $\sigma^0_{zz} = A\tau$, where A is the ratio of the zero-field conductivity to τ. A plot of interlayer resistivity versus $1/\sqrt{\tau}$ is shown in figure 2 for different values of ω_0. The interlayer resistivity is a non-monotonic function of τ. It will be seen below that this leads to non-monotonic temperature dependence.

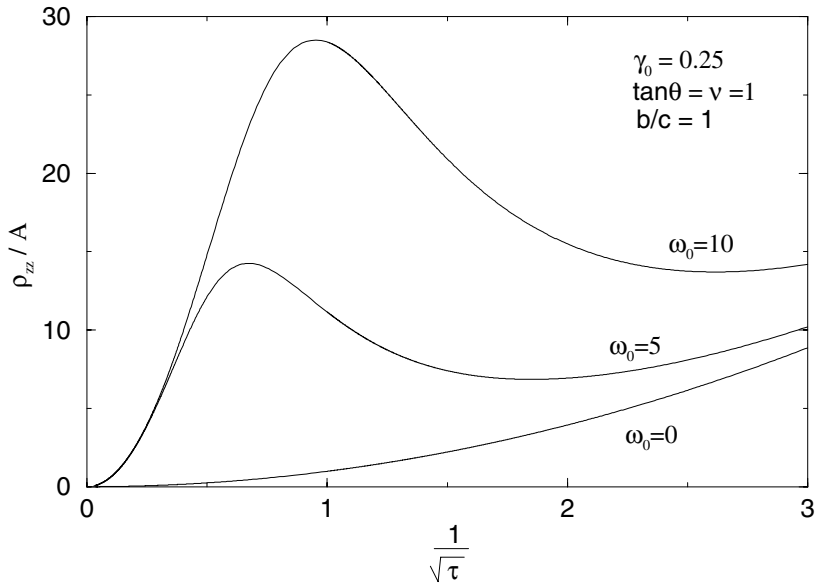

Figure 2. The non-monotonic dependence of the interlayer resistivity, at the $\nu = 1$ magic angle, on the scattering time τ. The curves shown are for $\gamma_0 = 0.25$ and for various values of ω_0, which is proportional to the magnetic field. $1/\sqrt{\tau}$ is used for the horizontal axis because it will be an increasing function of temperature in a Fermi liquid. A local minimum occurs at $\omega_0\tau \simeq 1/\sin\theta_1$ and there is a local maximum when $\omega_0\tau \simeq 2/(\gamma_0\sin\theta_1)$. The interlayer resistivity ρ_{zz} is normalized to $1/A$, where A is a constant equal to the ratio of the zero-field conductivity to the scattering time τ.

We now find for what values of τ the maxima and minima seen in figure 2 occur. Finding the extrema of equation (25) as a function of τ gives that a minimum occurs when

$$\omega_{c0}\tau \simeq \frac{1}{\sin\theta_1} \tag{26}$$

and a maximum occurs when

$$\omega_{c0}\tau \simeq \frac{2}{\gamma_0 \sin\theta_1}. \tag{27}$$

If $\gamma_0 \ll 1$, then the maximum will only be observed at sufficiently high fields and in high-purity samples.

4.2. The second magic angle ($\nu = 2$)

To obtain the interlayer conductivity for the second magic angle, a similar argument to that given above leads to

$$\sigma_{zz}(\theta_2) \simeq A\tau\left[\frac{1}{1+(\tau\omega_c)^2} + \left(\frac{\gamma_0 \tan\theta_2}{2}\right)^2\left(\frac{1}{1+(\tau\omega_c/2)^2} + \frac{1}{1+(3\tau\omega_c/2)^2}\right) + \frac{(\gamma_0\tan\theta_2)^4}{64}\right] \tag{28}$$

where we have set $\omega_c = 2\omega_b$ and θ_2 is the $\nu = 2$ magic angle. For small γ_0, the minima are again given by $\omega_c\tau \simeq 1$. To find the maxima we expand the first two terms in (28) to fourth order in $1/(\tau\omega_c)^2$. A maximum occurs when

$$\omega_{c0}\tau \simeq \frac{4}{\sin\theta_2(\gamma_0\tan\theta_2)^2}. \tag{29}$$

Since this is smaller than (27) by a factor of $1/\gamma_0$, in order to see such a maximum, even higher fields and lower temperatures will be required than for a maximum associated with the first magic angle.

4.3. Conductivity as $\theta \to 90^\circ$

We can expand the term

$$\left(\frac{1}{1+\tau^2(\omega_c - \omega_b\nu)^2} + \frac{1}{1+\tau^2(\omega_c+\omega_b\nu)^2}\right)$$

in the summation in (21) to second order in $\nu\cos\theta$ to obtain

$$\frac{2}{1+a^2}(1+\nu^2\cos\theta^2 A + \cdots) \tag{30}$$

where $a = \omega_0\tau$ and

$$A = \frac{a^2(3a^2-1)}{(1+a^2)^2} \approx 3$$

for $\omega_0\tau \gg 1$. Substitution of this into the conductivity gives

$$\frac{\sigma_{zz}(\theta \to 90^\circ)}{\sigma^0_{zz}} \simeq \frac{1}{(\omega_0\tau)^2}\left[J_0(\gamma_0\tan\theta)^2 + 2\sum_{\nu=1}^{\infty} J_\nu(\gamma_0\tan\theta)^2(1+3\nu^2\cos\theta^2+\cdots)\right]. \tag{31}$$

This can be simplified using the identities

$$\begin{aligned}\sum_{n=-\infty}^{\infty} J_n(z)^2 &= 1\\ \sum_{n=-\infty}^{\infty} n^2 J_n(z)^2 &= z^2/2\end{aligned} \tag{32}$$

to give

$$\frac{\rho_{zz}(\theta = 90^\circ)}{\rho^0_{zz}} \simeq \frac{(\omega_{c0}\tau)^2}{1 + 3\gamma_0^2}. \tag{33}$$

The resistivity is quadratic in the field as for the case of a linear dispersion, but the coefficient is smaller. This is consistent with figure 1 which shows that the resistivity near 90° does decrease with increasing γ_0. This field dependence is quite different to what is observed in the $(TMTSF)_2X$ materials. For $(TMTSF)_2ClO_4$ at 6.0 kbar [17] a linear field dependence is observed at high fields. In $(TMTSF)_2PF_6$ at pressures from 6 to 10 kbar, the resistivity saturates as the field increases [7, 18]. However, caution is in order because derivation of the quadratic dependence involved assuming that $t_c \tan\theta \ll t_b$ and so we only expect a quadratic dependence slightly away from 90° or in the limit $t_c \to 0$.

4.4. The Fermi-liquid model for the temperature dependence

We now consider a specific model for the temperature dependence of the scattering time τ. In a Fermi liquid the scattering rate, at temperatures much less than the Fermi temperature, has a temperature dependence of the form [26, 32]

$$\frac{1}{\tau} = \frac{1}{\tau_0} + \beta T^2 \tag{34}$$

where the first term is due to impurity scattering and the second is due to electron–electron scattering. Using this expression for τ in equation (25), we can now plot the temperature dependence of the resistivity. This is shown in figure 3 for various values of $\omega_{c0}\tau_0$. The resistivity is not a monotonic function of temperature but has a minimum when $\omega_c\tau(T) \sim 1$.

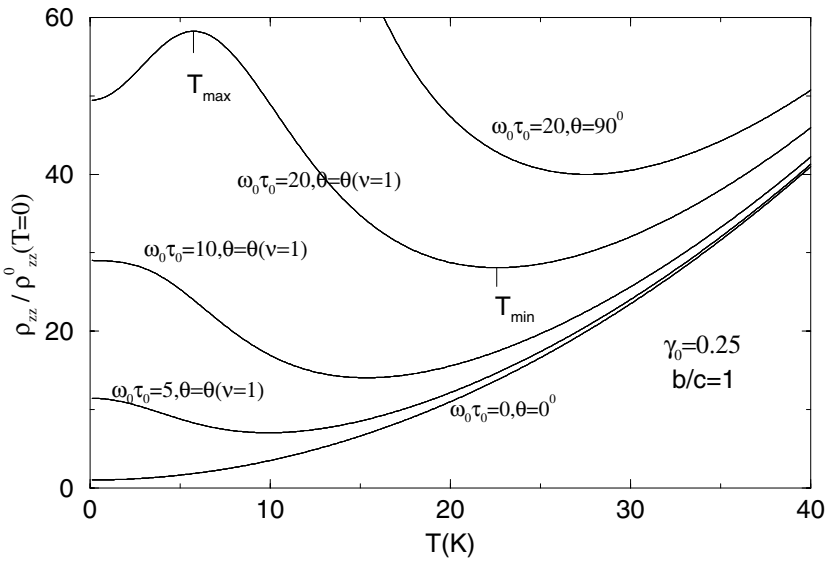

Figure 3. The non-monotonic dependence of the interlayer resistivity, at the $\nu = 1$ magic angle, on temperature. A Fermi-liquid form for the temperature dependence of the scattering rate is assumed. A value of $\tau_0\beta = 0.025\ \mathrm{K}^{-2}$ is used in equation (34) so that the temperature dependence of the zero-field resistivity roughly corresponds to that of typical samples of Bechgaard salts. At a temperature T_{min} defined by $\omega_0\tau(T_{min}) \simeq 1$, there is a minimum in the resistivity. For sufficiently high fields there is a temperature T_{max} at which the resistivity is a maximum.

If the field is sufficiently high, there is also a maximum. Using (34) we see that the minimum occurs at a temperature

$$T_{min} \simeq \left(\frac{\omega_{c0} \sin\theta}{\beta} \right)^{1/2}. \tag{35}$$

If $T_{max}^2 \gg 1/(\beta\tau_0)$, then (27) implies

$$T_{max} \simeq \left(\frac{\omega_{c0}\gamma_0 \sin\theta \tan\theta}{2\beta} \right)^{1/2}. \tag{36}$$

We are unaware of any measurements of the temperature dependence of the interlayer magnetoresistance of $(TMTSF)_2ClO_4$ at the magic angles. Although the temperature dependence at the $\nu = 1$ magic angle shown in figure 3 is similar to that reported in reference [7] for the *intralayer* resistance of $(TMTSF)_2PF_6$ at 9 kbar, the observed temperature dependence of the interlayer magnetoresistance is different [33]. It depends weakly on the temperature from 15 K down to about 3 K and then decreases.

The temperature dependence shown in figure 3 is for $\theta = 90^\circ$, i.e., the magnetic field is aligned with the $\boldsymbol{b}$-axis. The temperature dependence is qualitatively similar to that observed for $(TMTSF)_2ClO_4$ at ambient pressure [34]. Again, qualitatively very different behaviour was observed [7] for $(TMTSF)_2PF_6$ at 10 kbar. There it was found that the in-field resistance had a temperature dependence similar to the zero-field resistance.

Zheleznyak and Yakovenko have given a heuristic argument as to the origin of the maximum and minimum temperatures seen in the intralayer resistance in reference [7], suggesting that metal–insulator and insulator–metal phase transitions occur as the temperature passes through these values [26]. They argue that $T_{min} \approx \omega_b \sim B$ and $T_{max} \approx t_c$ which is independent of the field. Above T_{min}, the system is a two-dimensional metal. Below T_{min}, a magnetic field causes the electron motion in the $\boldsymbol{b}$-direction to be quantized resulting in a one-dimensional dispersion and correlations producing insulating behaviour. Below T_{max}, the interlayer coupling becomes important and metallic behaviour is recovered. In contrast, we find that T_{min} and T_{max} are given by (35) and (36), respectively, and both scale with $\sqrt{B}$. Careful measurements should be able to distinguish between these two different field dependences.

5. Conclusions

This paper only considers the interlayer resistivity ρ_{zz}, whereas magic angle effects are also seen experimentally in the intralayer resistivity ρ_{xx}. Maki pointed out [19] that the semi-classical theory will only give resonances in ρ_{xx} of order $(t_c/t_a)^2$, whereas they are observed to be much larger. A possible way around this problem is that experiments that are meant to measure ρ_{xx} may actually be measuring some of ρ_{zz}. This is because in highly anisotropic metals it is difficult to arrange the contacts and current path such that it lies completely within the layers. This potential problem increases the motivation to make thin-film samples of these metals.

It has been shown that within semi-classical transport theory, a non-linear dispersion parallel to the chains is necessary to produce dips in the interlayer magnetoresistance at integer magic angles. If the field direction is fixed at one of the magic angles, then one observes both minima and maxima in the temperature dependence of the interlayer magnetoresistance. This arises from the temperature dependence of the scattering rate. Since these maxima and minima can exist within a Fermi-liquid model, one should be cautious about associating them with non-Fermi-liquid behaviour or metal–insulator transitions. On the other hand,

although the Fermi-liquid model considered here gives a good description of many of the properties of $(TMTSF)_2PF_6$ at pressures from 6 to 8 kbar and of $(TMTSF)_2ClO_4$, it gives a poor description of their properties when the field is parallel to the layers and of the intralayer transport. Qualitatively very different behaviour is observed in $(TMTSF)_2PF_6$ at pressures of about 10 kbar; explaining it remains a considerable theoretical challenge.

Acknowledgments

This work was supported by the Australian Research Council. We thank P M Chaikin and M J Naughton for very helpful discussions. We also thank P M Chaikin for sending us unpublished experimental data.

References

[1] Ishiguro T, Yamaji K and Saito G 1998 *Organic Superconductors* 2nd edn (Berlin: Springer)
[2] Wosnitza J 1996 *Fermi Surfaces of Low Dimensional Organic Metals and Superconductors* (Berlin: Springer)
[3] For a recent experimental review, see
Liang W Y 1998 *J. Phys.: Condens. Matter* **10** 11 365
[4] McKenzie R H 1998 *Comment. Condens. Matter Phys.* **18** 309
[5] Bourbonnais C and Jerome D 1999 *Preprint* cond-mat/9903101
[6] Danner G M and Chaikin P M 1995 *Phys. Rev. Lett.* **75** 4690
[7] Chashechkina E I and Chaikin P M 1998 *Phys. Rev. Lett.* **80** 2181
[8] Danner G M, Kang W and Chaikin P M 1994 *Phys. Rev. Lett.* **72** 3714
[9] Lebed A G 1986 *Pis. Zh. Eksp. Teor. Fiz.* **43** 137 (Engl. Transl. 1986 *JETP Lett.* **43** 174)
[10] Boebinger G S, Montambaux G, Kaplan M L, Haddon R C, Chichester S V and Chiang L Y 1990 *Phys. Rev. Lett.* **64** 591
[11] Lebed A G and Bak P 1989 *Phys. Rev. Lett.* **63** 1315
[12] Naughton M J, Chung O H and Chaparala M 1991 *Phys. Rev. Lett.* **67** 3712
[13] Osada T, Kawasumi A, Kagoshima S, Miura N and Saito G 1991 *Phys. Rev. Lett.* **66** 1525
[14] Kang W, Hannahs S T and Chaikin P M 1992 *Phys. Rev. Lett.* **69** 2827
[15] Osada T, Kagoshima S and Miura N 1996 *Phys. Rev. Lett.* **77** 5261
Lebed A G and Bagmet N N 1997 *Phys. Rev.* B **55** 8654
Lee I J and Naughton M J 1998 *Phys. Rev.* **57** 7423
[16] Danner G, Kang W and Chaikin P M 1994 *Physica* B **201** 442
[17] Chashechkina E I and Chaikin P M 1997 *Phys. Rev.* B **56** 13 658
[18] Lee I J and Naughton M J 1998 *Phys. Rev.* B **58** R13 343
[19] Maki K 1992 *Phys. Rev.* B **45** 5111
[20] Osada T, Kagoshima S and Miura N 1992 *Phys. Rev.* B **46** 1812
[21] Blundell S J and Singleton J 1996 *Phys. Rev.* B **53** 5609
[22] Chaikin P M 1992 *Phys. Rev. Lett.* **69** 2831
[23] Moses P and McKenzie R H 2000 *Preprint* cond-mat/0006435
[24] Yakovenko V M 1992 *Phys. Rev. Lett.* **68** 3607
[25] Strong S P, Clarke D G and Anderson P W 1994 *Phys. Rev. Lett.* **73** 1007
Clarke D G and Strong S P 1997 *Adv. Phys.* **46** 545
Clarke D G, Strong S P, Chaikin P M and Chashechkina E I 1998 *Science* **279** 2071
[26] Zheleznyak A T and Yakovenko V M 1999 *Eur. Phys. J.* B **11** 385
[27] McKenzie R H, Qualls J S, Han S Y and Brooks J S 1998 *Phys. Rev.* B **57** 11 854
[28] Qualls J S, Brooks J S, Uji S, Terashima T, Terakura C, Aoki H and Montgomery L K 2000 *Preprint* cond-mat/0005202
[29] Ashcroft N W and Mermin N D 1975 *Solid State Physics* (Philadelphia, PA: Saunders)
[30] McKenzie R H and Moses P 1998 *Phys. Rev. Lett.* **81** 4492
[31] Hanasaki N, Kagoshima S, Hasegawa T, Osada T and Miura N 1998 *Phys. Rev.* B **57** 1336
[32] Gorkov L P 1996 *J. Physique* I **6** 1697
Gorkov L P and Mochena M 1998 *Phys. Rev.* B **57** 6206

In a quasi-two-dimensional system there are logarithmic corrections to (34). However, such corrections have no qualitative effect on the results presented here.

[33] Chashechkina E I and Chaikin P M 1999 *Synth. Met.* **103** 2176

[34] Danner G M, Ong N P and Chaikin P M 1997 *Phys. Rev. Lett.* **78** 983

At low temperatures, ρ_{zz} reaches a maximum value, contrary to the case for figure 3. However, this maximum can be interpreted as due to the presence of a high-field superconducting state; see

Naughton M J, Lee I J, Danner G M and Chaikin P M 1997 *Synth. Met.* **85** 1481